heritage

MDPI

Article

An Archaeometric Investigation of Gems and Glass Beads Decorating the Double-Arm Reliquary Cross from Liège, Belgium

Yannick Bruni [1], Frédéric Hatert [1,*], Merry Demaude [1], Nicolas Delmelle [1], Philippe George [2] and Julien Maquet [3]

1 Laboratory of Mineralogy, University of Liège B18, B-4000 Liège, Belgium; yannick.bruni@uliege.be (Y.B.); merry.demaude@uliege.be (M.D.); nicolas.delmelle@uliege.be (N.D.)
2 Rue Maghin 64, B-4000 Liège, Belgium; philippe.george@tresordeliege.be
3 Liège Treasure of the Cathedral, Rue Bonne Fortune 6, B-4000 Liège, Belgium; julien.maquet@tresordeliege.be
* Correspondence: fhatert@uliege.be

Abstract: In 1914, a magnificent reliquary cross dating from the early XIIIth century was discovered in a safe from the Liège Cathedral. This double-arm cross shows a wooden structure, covered by gold-coated copper on the front, and by carved silver plates on the back. Its total length is 34 cm, and it is covered by filigrees, gems, glass beads, and pearls on its front. The reliquary cross was analysed by Raman spectrometry and X-ray fluorescence spectrometry (pXRF) to determine the mineralogical and chemical compositions of gems, glass beads, and metals that have been used to decorate it. The results confirm the identification of twenty-five turquoises from Egypt, one garnet from Sri Lanka, as well as six quartz and one opal whose origin is difficult to certify. Twelve glass beads, showing green, blue, or amber tints, were also identified. Their compositions either correspond to soda lime glasses with natron or to potash–lead glasses similar to those of Central Europe. Moreover, a small polished red cross and a green stone appear to be constituted by nice doublets, composed of coloured glass covered by quartz. The filigrees contain Au and Cu, while carved plates covering the edges and the back of the cross are made of silver.

Keywords: double-arm reliquary cross; Liège; Belgium; gems; glass beads; Raman; pXRF

Citation: Bruni, Y.; Hatert, F.; Demaude, M.; Delmelle, N.; George, P.; Maquet, J. An Archaeometric Investigation of Gems and Glass Beads Decorating the Double-Arm Reliquary Cross from Liège, Belgium. *Heritage* **2021**, *4*, 4542–4557. https://doi.org/10.3390/heritage4040250

Academic Editor: Emeline Pouyet

Received: 6 October 2021
Accepted: 17 November 2021
Published: 30 November 2021

1. Introduction

The double-arm reliquary cross from Liège is hosted in the Treasure of the Cathedral. A detailed investigation by George [1] showed that this goldsmithery item was realized with a "Mosan style" (name from the Meuse River located nearby) during the early XIIIth century. The history of this magnificent artwork is quite unknown because Émile Schoolmeesters, dean of the Chapter, discovered it inside a safe of the Treasure only in 1914. Initially assigned to Hugo d'Oignies or its workshop, the cross, measuring 34 cm height, is made of a wood structure, covered by golden copper filigrees and decorated by stones on its front (Figure 1A,B), and by carved silver plates on its edges and back (Figure 1B,C). The two cavities on the back contained some relics of the Holy Cross, now disappeared. Fifty-six stones with various colours and shapes, and showing cabochon cuttings, decorate the cross. In 1993, a restoration allowed to Louis-Pierre Baert to remove the more recent golden copper pedestal and to add two new missing stones [1–3].

The interest of analysing ancient goldsmiths' artwork using modern archaeometric methods has increased recently, as shown by the recent Raman and XRF investigations of the reliquary from Lierneux [4], of the "Sainte-Épines" crown from Namur [5], and of the reliquary-bust of Saint Lambert from Liège [6]. The reliquary cross investigated herein was previously analysed by Demaude [2] using portable Raman spectrometer and qualitative p-XRF. The aim of the present paper is consequently to complete this preliminary study by using quantitative X-ray fluorescence methods. The chemical data collected on the glass

beads will allow to determine the origin of the raw materials, the colouring methods used, and the period of manufacture, while the results obtained on gemstones will help us to shed some light on their nature and their original sources. Such new archaeometric data are helpful to determine the commercial links between Liège and the neighbouring countries during the 12th and 13th centuries.

Figure 1. Photographs of the reliquary cross from Liège. (**A**) Front view. (**B**) Front side view. (**C**) Zoom on the lateral silver plate.

2. Materials and Methods

The reliquary cross is a precious artwork that cannot be damaged or moved outside the Treasure of Liège. Its entire surface is decorated by fifty-six stones showing various colours, shapes, and always a cabochon cutting. Raman and X-ray fluorescence spectrometries are therefore the best techniques to study this item, because they are portable and non-destructive.

The portable Raman spectrometer used in our analyses is an Enwave Optronics EZRAMAN-I-DUAL, loaned by the European centre of Archaeometry of Liège, Belgium. This optic-fibre based instrument is equipped with two light sources: a green Nd:YAG laser (532 nm) and a red diode source (785 nm). The spot diameter of the optic fibres is approximately 6 mm, and the detector is of CDD type. A removable rubber tip is attached to their end of the probe to protect the beam from ambient light and to always keep a relatively constant sample-probe distance during repeated measurements. The output power of the spectrometer can be adjusted to a maximal value of 400 and 100 mW for the 785 and 532 nm wavelengths, respectively; only 10% of the maximal power was used in our study (10 to 40 mW). The spectral region covered was between 100 and 3200 cm^{-1} for the 785 nm diode, and between 100 and 4000 cm^{-1} for the 532 nm laser. Consequently, spectral resolutions are different, namely 7 or 8 cm^{-1}, for the 785 and 532 nm sources, respectively. Duration of analysis was of 60 to 120 s. Raman spectra were recorded in the software in *.txt format and then exported in Excel. The final spectra were cut at 1400 cm^{-1} (spectral region between 100 and 1400 cm^{-1}) for a better presentation, and they were not affected by any post-acquisition data manipulation.

The portable X-ray fluorescence spectrometer (pXRF) is a Thermo Fischer Niton XL3t, equipped with a 'GOLDD' detector and a 3 mm spot diameter, from the Mineralogy Laboratory, University of Liège (Belgium). X-rays are produced with a silver anode, using an acceleration voltage of 50 kV and a current of 200 μA. The lightest detectable element is Mg, but without a helium flow, this element cannot be detected with a good accuracy. The standardization mode selected is the "Cu/Zn Mining", which includes all elements of interest for an archaeometric study (e.g., K, Ca, Si, Mn, Fe, and Pb). This procedure uses successively four separate filters to determine the concentrations in percentage of each chemical elements: a high filter (15 s counting time), a main filter (15 s), a low filter (15 s), and a light filter (30 s), leading to a total counting time of 75 s per analysis point. The software utilizes a Fundamental Parameters algorithm to determine concentrations of each element. The data obtained from the XLT3 were downloaded to a computer for analysis. They were then multiplied according with a standard element oxide conversion table to produce a percentage by weight of each oxide. Finally, the values were normalized to 100 wt%, after addition of the Na_2O and H_2O values estimated from the literature.

Reference materials have been analysed (glass pearls JCH-1, GSP-1, SARM-39, and BX-N [7] and pure metals Ag, Au, and Cu), in order to determine the precision and accuracy of the pXRF instrument. Six point analyses were realized on different spots on these standards. For the metals, the precision of these measurements can be estimated at around 5%, and the accuracy below 2%. For the glasses, the values strongly depend on the atomic weight of the elements. Magnesium and aluminium are not very precise nor accurate; for this reason, the values for Mg in Table 1 are rounded to the unit. Elements with higher atomic weights, and occurring above 1 wt. % in the standards, show good precisions generally below 5%, as well as fairly good accuracies below 20%. Table S1 contains the results of these standards analyses.

3. Results

3.1. Visual Description of Stones and Pearls

The reliquary cross of Liège is decorated by fifty-six coloured stones and pearls, which are symmetrically arranged (Figures 1 and 2). They show various colours (green, blue, turquoise, white, amber, grey, purple, or red) and shapes (rectangular, cross, oval, or round), but always a cabochon cutting (Figure 3).

Turquoise is the dominant colour with twenty-seven stones (e.g., n° 1, 9, 10—Figure 2A), situated at all flowered ends (18 stones) and at different positions on the handle (nine stones) (Figure 1). These decorative elements always show a rounded shape with a diameter of 4 to 5 mm, except for the central ones (around the red cross) that measure approximately 8 × 5 mm (Figure 3F). The small turquoise "R2" (Figure 2B), located at the bottom left of the handle between the white (n° 16) and the blue (n° 17) stones, has been added during the restoration in 1993 [1].

Six small pearls are positioned in pairs just before the two flowered ends of the longer crossbar, as well as at the bottom of the handle. They have a pearly white colour, a spherical shape, and a diameter around 4 mm. The pearl "R1" (Figure 2B), located at the bottom left of the crossbar, is a new sample dating from the restoration [1].

Eight green stones adorn the cross: six large ones (n° 2, 5, 6, 14, 18, 19) located at each centre of flowered ends, as well as two small ones located on the handle (called "a" and "b"; Figure 2B). The stone n° 18 shows a rectangular shape (13 × 10 mm) with an inhomogeneous green colour, bubbles, and cracks (Figure 3D). It is certainly constituted by a doublet, partly decomposed in the separation, composed of a dark base covered by a colourless upper part, but the setting prevents a good visibility. The other large green beads are oval (11 × 8 mm), often with bubbles and cracks, and consist of doublets with a colourless base and a green upper part.

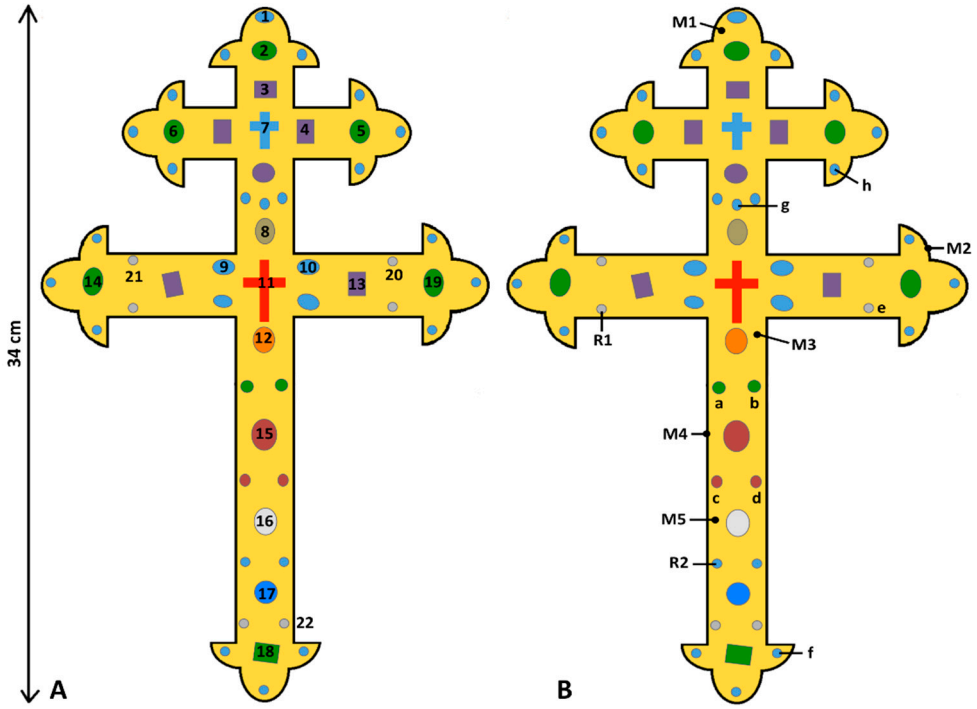

Figure 2. (**A,B**) Localisation and numbering of the different decorative elements on the reliquary cross from Liège.

The cross is also decorated by one amber, one deep blue, one grey, six purple, one white, and three dark red stones, as well as by two transparent crosses with light blue and red colours. The amber (n° 12) and blue (n° 17) beads, located on the lower handle, show an oval shape (12 × 10 mm) composed of nice colourless/amber (or blue) doublets, with some glue traces and small gas bubbles in the upper coloured part (Figure 3E). Higher on the cross, the grey cabochon (n° 8), looking like a smoky quartz, shows a rounded shape (17 × 12 mm), without any inclusions (Figure 3F). The six purple stones (e.g., n° 3, 4, 13), situated around the little blue cross (four stones) and on the second longer crossbar (two stones), show rectangular shapes (11 × 8 mm), except the sample below the blue cross (10 mm), which is rounded (Figure 3G). Their colour and homogeneity indicate that they certainly correspond to amethyst. The white stone (n° 16), above the blue one (n° 17), shows an oval shape (12 × 10 mm), with a slight play-of-colour dominated by blue colour, looking like a precious opal (Figure 3A). Still above on the cross, three dark red cabochons (n° 15, c and d), one large oval (14 × 11 mm) and two small rounded (5 mm), also decorate the handle (Figure 3B). According to Demaude [2], the two small stones could have some gas bubbles inside, therefore corresponding to a glass bead. Finally, two transparent crosses, positioned at the two intersections between the handle and the crossbars, can be observed. The first one (n° 7), measuring 19 × 16 mm, shows a doublet composed of a colourless base surmounted by a light blue stone (Figure 3H), whose colouring seems to be irregular. The second cross (n° 11), measuring 27 × 17 mm, has a red colour when looking from above (Figure 3F) but a colourless aspect with a grazing light (Figure 3C).

3.2. Raman Spectroscopy

It was impossible to analyse all samples using Raman spectrometry, because some of them show too-small sizes compared to the spot diameter of the instrument, and some analyses were omitted due to their poor quality. A list of the Raman bands observed on the gemstones is available in Table 1.

Figure 3. Detailed pictures of some decorative elements occurring on the reliquary cross. (**A**) Rounded opal showing a nice iridescence n° 16. (**B**) Rounded red garnet n° 15. (**C**) Red cross composed of colourless quartz on the doublet top part n° 11. (**D**) Green glass bead with a discolouration and many gas bubbles n° 18. (**E**) Orange glass bead showing a gas bubble and a doublet n° 12. (**F**) Photograph with four turquoises n° 9–10, one smoky quartz n° 8, and one red cross n° 11. (**G**) Rounded amethyst located below the blue cross. (**H**) Visible doublet on the blue cross n° 7.

The green, blue, and amber stones show Raman spectra characterized by very large bands, located around 300–600 cm^{-1} (symmetric bending of SiO_4 tetrahedra) and 900–1300 cm^{-1} (Si-O stretching vibrations) [8]. These spectra are characteristic of amorphous glass material, as frequently observed in medieval goldsmithery items [4–6].

The dark red cabochon (n° 15) shows a spectrum with an intense peak at 908 cm^{-1}, as well as weak peaks at 340 and 540 cm^{-1} (Figure 4A), corresponding to almandine or pyrope-almandine spectra [9,10]. The spectra of the turquoise stones (n° 1, 9, 10) are characterized by a weak band around 1046 cm^{-1}, and the spectra of the pearls (n° 20–22,

R1) show bands at 690 and 1082 cm^{-1}, in good agreement with the Raman spectra of turquoise and aragonite, respectively [9,11–13] (Figure 4A).

Table 1. List of the Raman peaks observed in the spectra of gemstones decorating the reliquary cross from Liège. Numbers in bold indicate the most intense bands.

Sample ID	Phase	Colour	Raman Peaks (cm^{-1})
1	Turquoise	Turquoise	**1046**
9	Turquoise	Turquoise	**1036**
10	Turquoise	Turquoise	**1042**
3	Quartz	Purple	120; 194; 372; **464**; 792
4	Quartz	Purple	124; 192; 374; **460**; 790
13	Quartz	Purple	122; 198; 376; **462**; 794
11	Quartz	Red	126; 194; 336; 380; **460**; 676; 780; 1148
18	Quartz	Green	124; 196; 330; 382; **460**; 670; 778; 1136
20	Pearl	White	696; **1084**
21	Pearl	White	690; **1082**
22	Pearl	White	694; **1086**
Mav3	Glass	Blue	324; 402; 514; 716; 866; 1050
15	Garnet	Red	340; 540; 842; **908**; 1028

The spectra of amethyst (n° 3, 4 13) and smoky quartz (n° 8) show a strong band around 460 cm^{-1}, as well as a weak band around 194 cm^{-1}, characteristic of quartz [9]. The spectra of the red cross (n° 11) and of the green doublet (n° 18) are also similar, thus indicating that the upper parts of these doublets are constituted by quartz (Figure 4B). The white cabochon with a nice opalescence (n° 16) shows a Raman spectrum with very broad bands [2], thus confirming its identification as amorphous opal.

The Raman data consequently confirm that the gemstones observed on the double-arm cross from Liège are amethyst, almandine garnet, turquoise, opal, rock crystal and smoky quartz, while the blue, amber, and green stones are different kind of glass beads. A few smaller stones were previously analysed by Raman spectrometry, indicating a lead glass composition for the two green stones "a" and "b" (Figure 2B), as well as for the two dark red cabochons "c" and "d". An artificial pearl "e", as well as three artificial turquoises ("f", "g", and "h"), were also observed [2].

3.3. Chemical Characterization by Portable X-ray Fluorescence Spectrometry

Chemical analyses were performed with a pXRF spectrometer on eighteen coloured stones, numbered 1 to 18, as well as on noble metals located on the front (M1, M3, and M5) and lateral (M2 and M4) parts (Figure 2B); the results are given in Tables 2 and 3. Some samples were not analysed due to their small size. The magnesium content is rounded to the unit because it is the lightest detectable element that could not be determined with more accuracy. Water and sodium were not directly measured by pXRF; consequently, these values were calculated. Vanadium, strontium, chromium, barium, zinc, arsenic, and bismuth were always below the detection limit.

Purple (n° 2, 3, 13) and grey stones (n° 8), as well as the red cross (n° 11), are characterized by 100 wt.% SiO_2 (Table 2); they consequently correspond to quartz varieties. The purple stones can be identified as amethyst, a purple variety of quartz, whose allochromatic colour is due to the irradiation of iron impurities from Fe^{3+} into Fe^{4+}. The grey cabochon is a smoky quartz, whose colour is caused by Al^{3+} impurities added to a natural irradiation process [14]. Concerning the red cross, this colour does not exist in natural quartz, and the observation in grazing light allows seeing that the top part of the cross is colourless (Figure 3C). This decorating element is therefore a doublet red glass/rock crystal (colourless quartz).

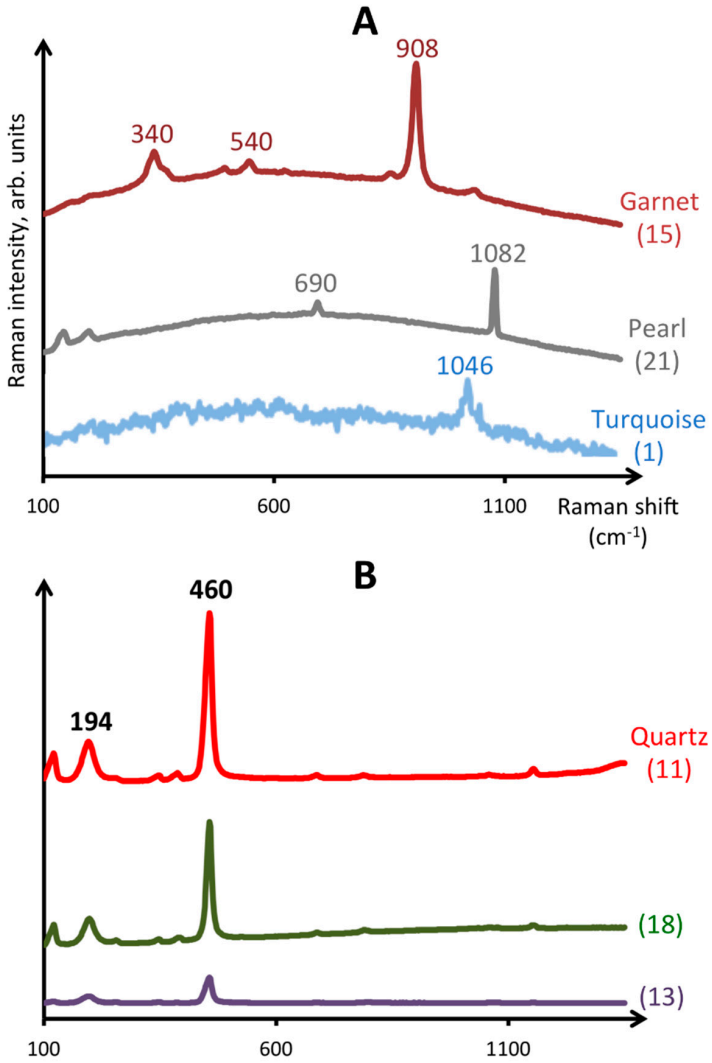

Figure 4. (**A**,**B**) Raman spectra of the gemstones decorating the reliquary cross from Liège. The colours of the spectra correspond to the observed colour of the stones, and the analysed samples are shown in parentheses.

The white cabochon (n° 16), showing a nice opalescence, reveals a chemical composition with high amount of SiO_2 (68.15 wt.%) and H_2O (31 wt.%), as well as small contents of Al_2O_3 (0.59 wt.%), CaO (0.19 wt.%), FeO (0.04 wt.%), and K_2O (0.03 wt.%), corresponding to opal (Table 2). The main substitutions in this mineral are the replacement of Si^{4+} by Al^{3+} and Fe^{3+}, compensated by monovalent or divalent cations as Ca^{2+} or K^+ [15].

Analysis of the dark red bead (n° 15) reveals high contents of SiO_2 (37.60 wt.%), Al_2O_3 (20.59 wt.%), and FeO (32.41 wt.%), as well as lower amounts of MgO (5 wt.%), CaO (3.79 wt.%), and MnO (0.79 wt.%) (Table 2). Such a composition corresponds to almandine garnet ($Fe_3Al_2Si_3O_{12}$), with significant pyrope ($Mg_3Al_2Si_3O_{12}$), grossular ($Ca_3Al_2Si_3O_{12}$), and spessartine ($Mn_3Al_2Si_3O_{12}$) components. Divalent iron (Fe^{2+}), located on the distorted cubic site of the garnet structure, gives its idiochromatic dark red colour.

The analyses of turquoise stones (n° 1, 9, 10) show values of 32–33 wt.% P_2O_5, 34–38 wt.% Al_2O_3, and 9–13 wt.% CuO (Table 2), in good agreement with the turquoise mineral, $CuAl_6(PO_4)_4(OH)_8.4H_2O$. Minor contents of SiO_2 (0.54 to 1.08 wt.%) and FeO (0.58 to 1.23 wt.%) are also observed. The idiochromatic sky blue colour is due to the divalent copper (Cu^{2+}), as well as the low content of iron giving greenish hues. Turquoises on the cross have therefore a sky-blue coloration, due to the level of iron below 0.7% FeO [14,16].

Table 2. Chemical composition of gems and glass beads decorating the cross from Liège.

Sample ID	Phase	Colour	H_2O [1]	Na_2O [2]	MgO [3]	Al_2O_3	SiO_2	P_2O_5	SO_3	Cl	K_2O	CaO	MnO	FeO	NiO	CuO	CoO	PbO	TiO_2	SnO_2	Sb_2O_3
3	Quartz	Purple	-	-	-	-	**100.00**	-	-	-	-	-	-	-	-	-	-	-	-	-	-
4	Quartz	Purple	-	-	-	-	**100.00**	-	-	-	-	-	-	-	-	-	-	-	-	-	-
13	Quartz	Purple	-	-	-	-	**100.00**	-	-	-	-	-	-	-	-	-	-	-	-	-	-
2	Glass	Green	-	-	-	1.59	**44.50**	**3.17**	1.45	0.76	**5.73**	0.30	0.16	0.54	0.11	1.71	-	**39.93**	0.02	-	0.03
5	Glass	Green	-	-	-	1.71	**35.06**	**2.31**	1.82	0.73	**6.46**	0.57	0.18	0.74	0.08	1.96	-	**48.31**	0.03	0.04	-
6	Glass	Green	-	-	-	1.28	**30.85**	1.44	0.72	0.34	**5.76**	0.83	0.17	0.86	0.12	**2.26**	-	**55.32**	0.04	-	-
14	Glass	Green	-	-	-	1.48	**42.27**	**2.37**	0.66	0.67	**4.92**	0.55	0.09	0.55	0.10	1.88	-	**44.44**	0.03	-	-
18	Quartz/glass	Green	-	-	-	0.25	**98.73**	0.59	0.15	-	-	-	-	-	-	0.27	-	-	0.02	-	-
1	Turquoise	Turquoise	**17**	-	-	**36.82**	1.08	**32.48**	0.90	-	0.08	0.23	-	0.58	-	**10.79**	-	-	-	0.02	-
9	Turquoise	Turquoise	**17**	-	-	**38.12**	0.64	**32.69**	1.28	-	0.12	0.21	-	0.63	-	**9.16**	-	-	-	0.11	-
10	Turquoise	Turquoise	**17**	-	-	**34.16**	0.54	**32.79**	1.02	-	0.07	0.21	-	1.23	-	**12.94**	-	-	-	0.04	-
7	Glass	Blue	-	-	-	1.22	**49.71**	1.15	1.88	0.52	**5.88**	**-**	0.25	-	0.09	0.20	0.05	**38.83**	0.03	-	0.19
17	Glass	Blue	-	**17**	-	1.75	**72.88**	0.12	0.56	-	0.25	**6.32**	0.13	0.09	0.06	0.35	0.04	0.31	0.02	0.03	0.08
11	Quartz/glass	Red	-	-	-	-	**100.00**	-	-	-	-	**-**	-	-	-	-	-	-	-	-	-
12	Glass	Amber	-	**17**	-	1.47	**70.42**	0.12	0.87	0.04	0.77	**8.84**	-	0.34	-	0.02	-	0.01	0.05	0.02	-
16	Opal	White	**31**	-	-	0.59	**68.15**	-	-	-	0.03	0.19	-	0.04	-	-	-	-	-	-	-
8	Quartz	Grey	-	-	-	-	**100.00**	-	-	-	-	**-**	-	-	-	-	-	-	-	-	-
15	Garnet	Red	-	-	**5**	**20.59**	**37.60**	-	-	-	-	**3.79**	0.79	**32.41**	-	-	-	-	0.04	-	-

Analyses realized by p-XRF, data presented as wt. % of oxides, normalized to 100 wt. %. -: Below detection limit. Percentages above 2 wt. % are shown in bold. [1]: H_2O values in turquoise and opal were calculated and rounded to the unit. [2] The Na_2O contents in samples 12 and 17 were constrained between 13 and 21 wt. % (average 17 wt. %), according to the literature data for such glasses [17–19]. [3]: MgO contents are rounded to the unit, due to the low precision and accuracy for this element.

The green, blue, and amber cabochons were identified visually and by Raman spectrometry as glass beads. The green stones (n° 2, 5, 6, 14), except one (n° 18), are composed of 40 to 55 wt.% PbO, 31 to 44 wt.% SiO_2 and 5 to 7 wt.% K_2O, with low contents of CuO (1.71 to 2.26 wt.%), Al_2O_3 (1.28 to 1.71 wt.%), Cl (0.34 to 0.76 wt.%), FeO (0.54 to 0.86 wt.%), CaO (0.30 to 0.83 wt.%), and MnO (0.09 to 0.18 wt.%) (Table 2). The green rectangular bead n° 18 shows another chemical composition with 98.73 wt.% SiO_2, 0.27 wt.% CuO, and 0.25 wt.% Al_2O_3, thus corresponding to quartz. This sample is certainly constituted by a quartz/green glass doublet, since no natural quartz shows this intense green colour. A discolouration, as well as many gas bubbles and cracks (Figure 2) and a fairly visible separation in the side view, confirm this hypothesis.

The light blue cross (n° 7) shows a composition with 49.71 wt.% SiO_2, 38.83 wt.% PbO, and 5.88 wt.% K_2O. Small amounts of Al_2O_3 (1.22 wt.%), MnO (0.25 wt.%), CuO (0.20 wt.%), and CoO (0.05 wt.%) are also observed. The blue cabochon located at the bottom of the handle (n° 17) contains very high contents of SiO_2 (72.88 wt.%) and CaO (6.32 wt.%), as well as lower amounts of Al_2O_3 (1.75 wt.%), CuO (0.35 wt.%), K_2O (0.25 wt.%), and CoO (0.04 wt.%). The amber cabochon (n° 12) is characterized by 70.42 wt.% SiO_2, 8.84 wt.% CaO, 1.47 wt.% Al_2O_3, 0.77 wt.% K_2O, and 0.34 wt.% FeO (Table 2).

The analyses of noble metals (Table 3) indicate that the filigrees (M1, M3, and M5) contain 50.23 to 68.38 wt.% Au, 26.14 to 43.53 wt.% Ag, and 2.90 to 6.18 wt.% Cu, thus confirming their gold composition. The lateral silvery plates (M2 and M4) are composed of approximately 92 wt.% Ag and 8 wt.% Cu.

Table 3. Chemical compositions of noble metals constituting the reliquary cross from Liège.

Sample ID	Ag	Au	Pb	As	Cu	Fe	Ni	Co
M1	26.14	68.38	-	-	5.47	-	-	-
M2	92.07	-	-	-	7.93	-	-	-
M3	43.59	50.23	-	-	6.18	-	-	-
M4	92.44	-	-	-	7.56	-	-	-
M5	39.52	57.58	-	-	2.90	-	-	-

Analyses realized by p-XRF, data presented as wt. % of elements, normalized to 100 wt. %. -: Below detection limit.

4. Discussion

4.1. Composition and Dating of Glass Beads

Coloured glass beads are used for a long time to imitate more expensive gemstones. They are manufactured from a mixture of three components: a source of silica (also called "former agent"), a flux, and a stabilizer, to which a colouring agent and/or an opacifier may be added. Sand was exclusively used as silica source until the 14th century, before being replaced by pure quartz pebbles because sand contained many impurities that may sometimes modify the colour (e.g., Ti, Al, and Fe). The flux, composed of sodium, calcium, and/or potassium, allows reducing the silica melting point. It was constituted by natron until the beginning of the Middle age and was then gradually replaced by plant and wood ashes. This replacement of natron was certainly due to the depletion of natron deposits and to political instabilities. The natron and coastal plant ashes produced soda–lime glasses, while continental plant ashes and wood generated potash–lime glasses. Finally, stabilizers (Mg, Al, and Ca) were added to decrease the glass solubility in water and to avoid devitrification. Moreover, antimony and manganese were often used as decolourizers, giving a totally transparent glass [20–26].

Lead glass was already known during the Roman times, but from about the 9th century, lead glass started to be more common in Europe and in the Islamic area [27,28]. This glass is made from a mixture of sand, lead, and pigments to eventually give a colour. Sometimes, ashes could also be added [27]. Lead allows increasing the shine of the stone, as well as to reduce the melting point at approximately 750 °C, compared to 1250 °C for ash glasses [21,27]. According to Mecking [27], European medieval lead glasses can be devised into five groups depending on their lead, calcium, and potassium contents: high lead glass

(PbO > 65 wt.%), lead smoother (PbO < 20 wt.%), wood–ash lead glass (CaO/K_2O = 1), Slavic lead glass (K_2O = 14 wt.%), and finally Central European lead–ash glass (CaO/K_2O between 0.009 and 0.36).

The kind of cutting technique can also be used for the dating of a stone. The cabochon polishing method, known since the 10th millennium BC, was generalized all around the world in the 4th century BC, due to technical improvements allowing the polishing of small stones. This cutting gives a nice colour to the stone and allows keeping a maximal amount of material. Simple faceting, composed of a large square or rectangular table surrounded by four facets, appeared in Europe during the Middle Ages and progressively became more complex from the 14th century [17,21,29].

The deep blue and amber cabochons, observed on the reliquary cross, contain high levels of SiO_2 and CaO, as well as low amounts of K_2O (Table 2); they are consequently constituted by soda–lime glass, with expected sodium concentration between 13 and 21 wt.% Na_2O [18,19,30]. Moreover, Raman spectra from Demaude [2] show peaks at 560 and 1072 cm^{-1}, thus confirming this hypothesis [31]. The former agent is composed of sand and the flux of natron, a natural evaporite material differentiated from ashes thanks to K_2O and MgO values below 1.5 wt.% (Figure 5A). This mineral, not available in Europe, was usually imported from the eastern Mediterranean, often already fused with sand [19,26,28,30,32]. The pXRF analyses also reveal the presence of other chemical elements, such as aluminium, titanium, iron, or antimony (Table 2). As natron contains very low amounts of impurities, minor and trace elements certainly originate from sand (Ti, Al, and Fe), decolouring (Mn and Sb) or colouring (Co, Cu, Fe, and Sb) agents (see below), and/or sometimes from recycling processes (Sb, Sn, Pb, Ni, and Cu) [19,33]. Soda–lime glasses with natron were exclusively used until the beginning of the Middle Age, before being gradually replaced by wood and plant ashes to almost disappear during the 13th century [20,25,27,28]. It was probably a shortage of natron due to political events, climate change, and/or a trade interruption that caused this transition. Around the 12th century, the recycling was mainly used for blue glass beads, with a mix between Roman blue tesserae and non-coloured glasses, generated by the scarcity of cobalt deposits until the 13th century [34]. The chemical compositions of these two samples, as well as their simple cabochon cuttings without polishing traces, seem to show that they are prior or contemporary to the cross manufacturing.

The small blue cross and the green stones, except the rectangular one (n° 18), are characterized by approximately 40 to 50 wt.% PbO, 30 to 50 wt.% SiO_2, and 5 to 6 wt.% K_2O (Table 2). This chemical composition corresponds to potash–lead glasses, probably with ashes since PbO values are below 55 wt.% [27]. Raman spectra [2] show peaks at about 430, 735, 950, and 1010 cm^{-1}, also confirming this interpretation [31]. Concerning their origin and dating, the PbO vs. CaO/K_2O diagram (Figure 5B) indicates that these samples are similar to Central European lead glasses dating from the Middle Age [27]. Indeed, lead glass beads from the 17th and 18th centuries generally contain higher potassium (9–16%) and lower lead (17–35%) amounts [35].

4.2. Colouring Agents Used in Glass Beads

The three colours listed for the glass beads decorating the Liège cross are green, amber, and blue. A colouring agent has been added to the molten glass, except for the light blue cross, where a dye bath has probably been used, as shown by the alteration and irregularities visually observed.

The deep green colour is due to a mixture of Cu^{2+} and Fe^{3+} [21,36], and the amber tint is due to a charge transfer between trivalent iron (Fe^{3+}) and dissolved sulphur (S^{2-}). Less than 0.2 wt.% of iron is enough to give that colour, if a reducing agent is also present in the mixture [21,37]. The deep blue cabochon, as well as the blue cross, are coloured by cobalt (0.05 wt.%), a strong colouring agent. A small amount of this element, below 0.05 wt.%, can already give an intense hue to a glass bead [21,38]. Cobalt used in European and Mediterranean glass production has been divided into three groups depending on their

sources, which contain different minor elements such as nickel, copper, and zinc [34,39,40]. Since no significant amounts of Zn (< LOD) and Ni (200 ppm) have been measured in our samples, famous German deposits (Erzebirge) discovered in the 13th and 16th centuries can already be excluded. The last sources concern cobalt associated with Cu, Mn, and Sb; this ore, probably used from the 12th century, was mined in the Near East (e.g., Iran). XRF analyses on blue samples show the presence of small amounts of copper, manganese, and antimony (Table 2), thus confirming this Near East origin [19,34].

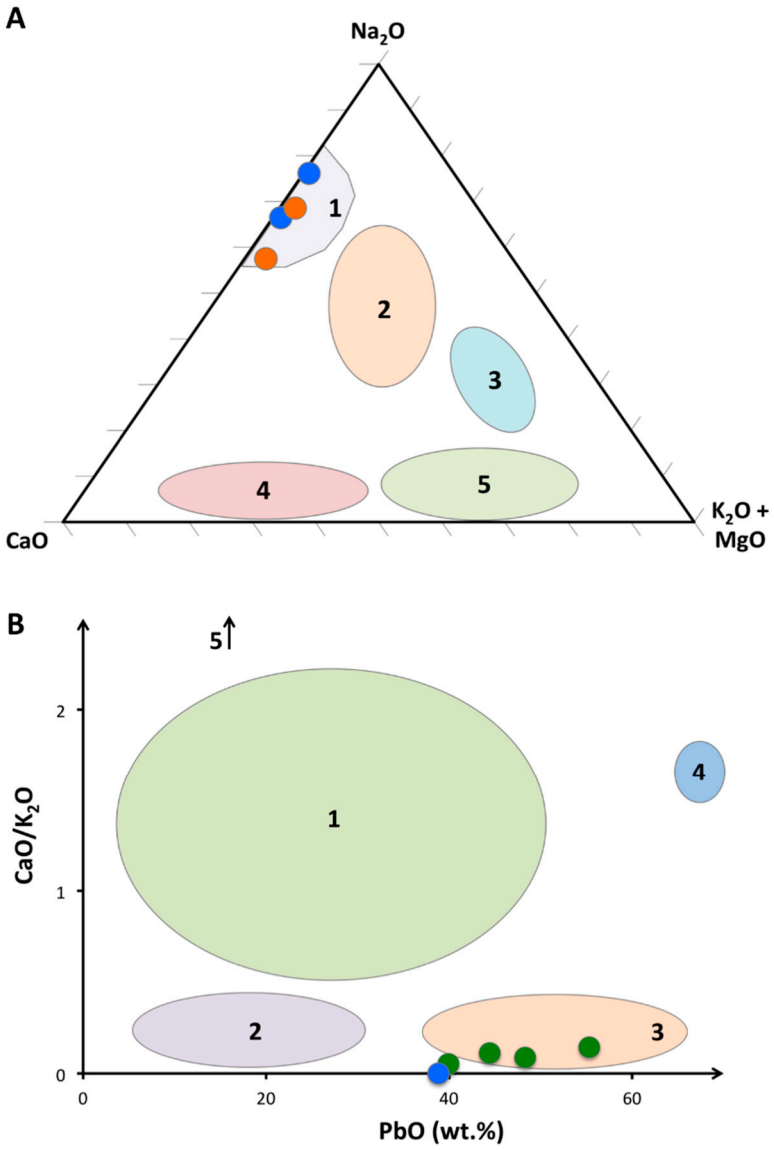

Figure 5. (**A**) Compositions of glass beads represented in the Na_2O-(K_2O+MgO)-CaO ternary diagram, used to determine the flux [18,19,30]. 1 = Soda–lime glass with natron; 2 = soda–lime glass with ashes; 3 = soda–potash glass; 4 = potash–lime glass; 5 = lime glass. The red and blue dots show the compositions of the amber and deep blue glass beads, respectively. (**B**) CaO/K_2O vs. PbO (wt.%) diagram showing the five types of lead glass beads. 1 = Wood–ash lead glass; 2 = Slavic lead–ash glass; 3 = Central European lead–ash glass; 4 = high lead glass; 5 = lead smoother. The green and blue dots represent the compositions of the green stones and of the blue cross, respectively.

4.3. Geographic Origin of Gemstones

The gemstones decorating the cross are amethyst, rock crystal (colourless quartz), smoky quartz, almandine garnet, turquoise, and "pearl" (constituted by aragonite). Best

quality samples were mainly imported from Asian countries as India, Sri Lanka, or Myanmar [41,42].

Garnet was one of the most common gemstones during the Middle Ages, appreciated for its deep red colour. Calligaro et al. and Gilg et al. [41–43] have classified garnets into, respectively, five "types" or six "clusters", depending on their origin. The garnet decorating the reliquary cross belongs to Type III (Figure 6A), corresponding to a Sri Lankan origin. According to the Fe_{tot}/CaO diagram [44], this sample is also very close to the Sri Lankan field, confirming this geographic origin (Figure 6B). Visually, Sri Lanka is a likely source considering the quality and size of the sample (Figure 3B), while European deposits could be directly excluded. However, almandine is a common mineral, with many consumed or lost sources around the world. A commercial trade road seems to connect Sri Lanka and India with the Mediterranean basin at the 13th century, even if few written documents mention this road [41,45,46].

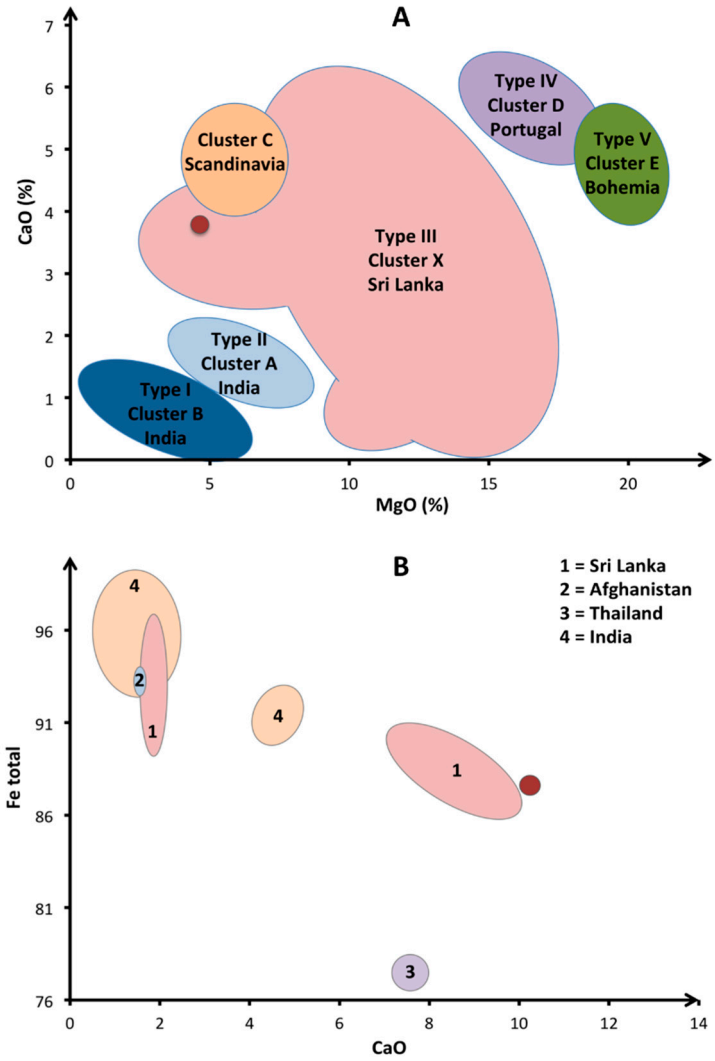

Figure 6. (**A**) Diagram showing the CaO and MgO contents of garnets from different origins. (**B**) The Fe and CaO contents of garnets from Asian deposits. The sample investigated herein is shown by a red dot.

Turquoise mines located in Egypt (Sinai), Iran (Nishapur, Kerman, and Damghan), and Central Asia (Uzbekistan/Afghanistan area) have been known since approximately the fourth millennium BC [47,48]. Chinese deposits, currently the most productive with those of United States, were only discovered during the 20th century [49], while European deposits are rarely marketable due to their greenish hue and porous aspect [48,50].

Carò et al. [47] compared Chinese, Egyptian, and Iranian turquoise sources by using two plots: Cu/Zn vs. Cu/Fe (Figure 7A) and Cu/Zn vs. Cu/As (Figure 7B). The three cabochons from the cross are close to (or included in) the Egyptian area. Central Asia does not appear because no reference specimens were collected there [47].

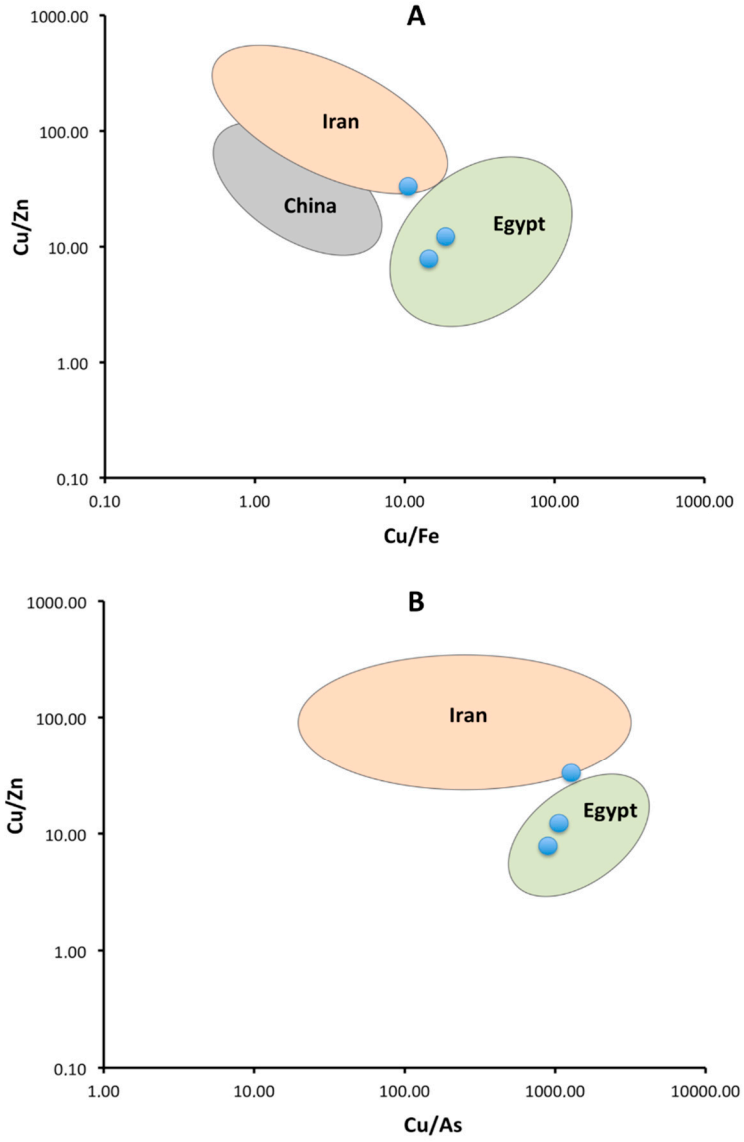

Figure 7. (**A**) Cu/Zn vs. Cu/Fe diagram showing three turquoise sources. (**B**) Cu/Zn vs. Cu/As diagram showing two turquoise sources located in Egypt and Iran. The blue dots represent the compositions of the samples investigated herein.

The three varieties of quartz on the cross are amethyst (purple), smoky quartz, and rock crystal (colourless), very cheap popular gems during the Middle Age [18,51]. These minerals were mined in many countries around the world, as for example France, Switzerland and Italy in Europe, Egypt in Africa, or Iran and India in Asia [52–54]. In the Middle Age, India was the main supplier of amethyst (Deccan basalts), using the same trade road as garnet, while nice smokey quartz and rock crystal could come from the Alps [2,29,55]. The exact origin is difficult to determine on isolated samples, since quartz does not contain significant trace elements [56].

One precious opal (n° 16), showing a slight play-of-colour, decorates the bottom of the Liège cross handle. The distinction between sedimentary and volcanic opals may be possible thanks to barium and REE (rare earth elements) concentrations, while Ca, Al, and

K contents allow the determination of their geographical origin [9]. Unfortunately, the high limit of detection for barium, around 350 ppm, and the REE contents, not measured with our pXRF, do not give us information about the formation environment of our opal. Concerning the deposit location, the Ca (1500 ppm), Al (3440 ppm), K (320 ppm), and Fe (330 ppm) values do not correspond to any opal published previously [8,57]. Historically, the only European source of precious gem opal in the Middle Age was the volcanic "Hungarian" deposits (Dubník mines), in eastern Slovakia today. Other known deposits, such as in Ethiopia, Australia, or Mexico, are impossible because all of them have only been discovered during the 19th and 20th centuries [58].

5. Conclusions

Dating from the beginning of the 13th century, the double-arm reliquary cross from Liège is decorated by fifty-six coloured samples, constituted by gemstones and glass beads showing simple cuttings. The filigrees mainly contain Au with few Ag and Cu, while lateral and back plates are made of pure silver. Gems found on the cross are almandine garnet, turquoise, quartz, opal, and pearls. Almandine originates from Sri Lanka, turquoise from Egypt, and opal probably from Slovakia. The origin of quartz is more difficult to establish from analytical data, but historically, it is likely that this mineral was imported from Indian or European deposits. Concerning glass beads, they show blue, green, or amber colours, and the chemical analyses reveal that deep blue and amber cabochons correspond to soda–lime glasses with natron, while green stones, except one, are similar to medieval potash–lead glasses from Central Europe. The small light blue cross also shows a potash–lead composition, and the red cross as well as one green stone is formed by a doublet composed of glass covered by quartz. All stones are probably contemporary with the reliquary cross, except the artificial pears and turquoises that certainly correspond to late repairs. The archaeometric investigation of religious goldsmith artwork, with non-destructive techniques like pXRF or Raman spectrometry, is a necessary step to better understand the historical and geographic contexts in which these objects were produced.

Supplementary Materials: The following are available online at https://www.mdpi.com/article/10.3390/heritage4040250/s1, Table S1: Results of the pXRF measurements realized on standard materials.

Author Contributions: The reliquary cross was loaned by P.G. and J.M., and P.G. also helped to write the historical context. M.D. performed a preliminary study of the cross, and the Raman data from this study are presented here. Y.B. performed the pXRF analyses, N.D. and F.H. helped for the Raman and pXRF analyses, and F.H. is the author of the photographs. The paper was mainly written by Y.B. and F.H. All authors have read and agreed to the published version of the manuscript.

Funding: This was founded by the Laboratory of Mineralogy, University of Liège (Belgium), and received no external funding.

Acknowledgments: Many thanks are due to three anonymous reviewers for their helpful comments during the review process.

Conflicts of Interest: The authors declare no conflict of interest.

References

1. George, P. Du prieuré d'Oignies au musée de Namur: Le binôme "reliques" et "arts précieux". A propos d'une croix inédite du trésor de la Cathédrale de Liège. *Trésor D'Oignies* **2013**, *23*, 136–153.
2. Demaude, M. Etude Gemmologique de Pièces D'orfèvrerie du Trésor de la Cathédrale Saint-Paul de Liège. Master's Thesis, University of Liège, Liège, Belgium, 2016; 81p.
3. Demaude, M.; Bruni, Y.; Hatert, F.; Strivay, D. Etude gemmologique de la croix-reliquaire à double traverse du Trésor de la Cathédrale de Liège. *Trésor Liège* **2017**, *50*, 9–15.
4. Bruni, Y.; Hatert, F.; George, P.; Strivay, D. An archaeometric investigation of glass beads decorating the reliquary of Saint Simètre from Lierneux, Belgium. *J. Archaeol. Sci. Rep.* **2020**, *32*, 102451. [CrossRef]
5. Bruni, Y.; Hatert, F.; George, P.; Cambier, H.; Strivay, D. A gemmological study of the reliquary crown of Namur, Belgium. *Eur. J. Miner.* **2021**, *33*, 221–232. [CrossRef]

6. Bruni, Y.; Hatert, F.; George, P.; Strivay, D. The Reliquary Bust of Saint Lambert from the Liège Cathedral, Belgium: Gemstones and Glass Beads Analysis by pXRF and Raman Spectroscopy. *Archaeometry* **2019**, *62*, 297–313. [CrossRef]
7. Govindaraju, K. 1994 compilation of working values and sample description for 383 geostandards. *Geostand. Newslett.* **1994**, *18*, 1–158. [CrossRef]
8. Robinet, L.; Bouquillon, A.; Hartwig, J. Correlations between Raman parameters and elemental composition in lead and lead alkali silicate glasses. *J. Raman Spectrosc.* **2008**, *39*, 618–626. [CrossRef]
9. RRUFF, 2021. An Integrated Database of Raman Spectra, X-Ray Diffraction and Chemistry Data for Minerals. Available online: https://rruff.info/ (accessed on 4 January 2021).
10. Culka, A.; Jehlička, J. A database of Raman spectra of precious gemstones and minerals used as cut gems obtained using portable sequentially shifted excitation Raman spectrometer. *J. Raman Spectrosc.* **2019**, *50*, 262–280. [CrossRef]
11. Wehrmeister, U.; Jacob, D.; Soldati, A.; Häger, T.; Hofmeister, W. Vaterite in freshwater cultured pearls from China and Japan. *J. Gemmol.* **2007**, *30*, 399–412. [CrossRef]
12. Karampelas, S.; Fritsch, E.; Makhlooq, F.; Mohamed, F.; Al-Alawi, A. Raman spectroscopy of natural and cultured pearls and pearl producing mollusc shells. *J. Raman Spectrosc.* **2020**, *51*, 1813–1821. [CrossRef]
13. Athavale, S.A.; Hambarde, M.S. Raman scattering: Fingersprint for identification of nature and color origin of pearls. *Intern. Res. J. Engeineer. Technol.* **2020**, *7*, 2065–2078.
14. Fritsch, E.; Rossman, G. An Update on Color in Gems. Part 2: Colors Involving Multiple Atoms and Color Centers. *Gems Gemol.* **1988**, *24*, 3–15. [CrossRef]
15. Gaillou, E.; Delaunay, A.; Rondeau, B.; Bouhnik-Le-Coz, M.; Fritsch, E.; Cornen, G.; Monnier, C. The geochemistry of gem opals as evidence of their origin. *Ore Geol. Rev.* **2008**, *34*, 113–126. [CrossRef]
16. Khorassani, A.; Abedini, M. A new study of turquoise from Iran. *Miner. Mag.* **1976**, *40*, 640–642. [CrossRef]
17. Klein, G. *Faceting History: Cutting Diamonds & Colored Stones*; Xlibris Corporation: Bloomington, IN, USA, 2005; 242p.
18. Schalm, O.; Janssens, K.; Wouters, H.; Caluwé, D. Composition of 12–18th century window glass in Belgium: Non-figurative windows in secular buildings and stained-glass windows in religious buildings. *Spectrochim. Acta Part B At. Spectrosc.* **2007**, *62*, 663–668. [CrossRef]
19. Tournié, A. Analyse Raman Sur Site de Verres et Vitraux Anciens: Modélisation, Procédure, Lixiviation et Caractérisation. Ph.D. Thesis, Université Pierre et Marie Curie, Paris, France, 2009; 162p.
20. Verità, M.; Renier, A.; Zecchin, S. Chemical analyses of ancient glass findings excavated in the Venetian lagoon. *J. Cult. Heritage* **2002**, *3*, 261–271. [CrossRef]
21. Cannella, A.-M. *Gemmes, Verre Coloré, Fausses Pierres Précieuses au Moyen Age. Le Quatrième Livre du Trésorier de Philosophie Naturelle des Pierres Précieuses de Jean d'Outremeuse*; Librairie Doz: Genève, Switzerland, 2006; 480p.
22. Tite, M.; Shortland, A.; Maniatis, Y.; Kavoussanaki, D.; Harris, S. The composition of the soda-rich and mixed alkali plant ashes used in the production of glass. *J. Archaeol. Sci.* **2006**, *33*, 1284–1292. [CrossRef]
23. Rasmussen, S.C. *How Glass Changed the World: The History and Chemistry of Glass from Antiquity to the 13th Century*; Springer: New York, NY, USA, 2016; 85p.
24. Verità, M. Secrets and innovations of Venetian glass between the 15th and 17th centuries: Raw materials, glass melting and artefacts. *Study Days Venetian Glass Approx.* **2014**, *172*, 53–68.
25. Neri, E.; Verità, M.; Biron, I.; Guerra, M.F. Glass and gold: Analyses of 4th–12th centuries Levantine mosaic tesserae. A contribution to technological and chronological knowledge. *J. Archaeol. Sci.* **2016**, *70*, 158–171. [CrossRef]
26. Phelps, M.; Freestone, I.C.; Gorin-Rosen, Y.; Gratuze, B. Natron glass production and supply in the late antique and early medieval Near East: The effect of the Byzantine-Islamic transition. *J. Archaeol. Sci.* **2016**, *75*, 57–71. [CrossRef]
27. Mecking, O. Medieval Lead Glass in Central Europe. *Archaeometry* **2013**, *55*, 640–662. [CrossRef]
28. Ares, J.D.J.; Schibille, N. Glass import and production in Hispania during the early medieval period: The glass from Ciudad de Vascos (Toledo). *PLoS ONE* **2017**, *12*, e0182129. [CrossRef]
29. Bariand, P.; Poirot, J.-P. *Larousse des Pierres Précieuses*; Larousse-Bordas: Paris, France, 1998; 288p.
30. Van Wersch, L.; Biron, I.; Neuray, B.; Mathis, F.; Chêne, G.; Strivay, D.; Sapin, C. Les vitraux alto-médiévaux de Stavelot (Belgique). *Archeo Sci.* **2014**, *38*, 219–234. [CrossRef]
31. Colomban, P.; Tournie, A.; Bellot-Gurlet, L. Raman identification of glassy silicates used in ceramics, glass and jewellery: A tentative differentiation guide. *J. Raman Spectrosc.* **2006**, *37*, 841–852. [CrossRef]
32. Costa, M.; Barrulas, P.; Dias, L.; Lopes, M.D.C.; Barreira, J.; Clist, B.; Karklins, K.; Jesus, M.D.P.D.; Domingos, S.D.S.; Vandenabeele, P.; et al. Multi-analytical approach to the study of the European glass beads found in the tombs of Kulumbimbi (Mbanza Kongo, Angola). *Microchem. J.* **2019**, *149*, 103990. [CrossRef]
33. Jackson, C.M.; Paynter, S.; Nenna, M.-D.; Degryse, P. Glassmaking using natron from el-Barnugi (Egypt); Pliny and the Roman glass industry. *Archaeol. Anthr. Sci.* **2018**, *10*, 1179–1191. [CrossRef]
34. Bidegaray, A.-I.; Pollard, A.M. Tesserae Recycling in the Production of Medieval Blue Window Glass. *Archaeometry* **2018**, *60*, 784–796. [CrossRef]
35. Dungworth, D.; Brain, C. Late 17th Century Crystal Glass: An Analytical Investigation. *J. Glass Stud.* **2009**, *51*, 111–137.
36. Wedepohl, K.H.; Krueger, I.; Hartmann, G. Medieval lead glass from northwestern Europe. *J. Glass Stud.* **1995**, *37*, 65–82.

37. Van Wersch, L.; Loisel, C.; Mathis, F.; Strivay, D.; Bully, S. Analyses of early Medieval stained window glass from the Mon-astery of Baume-Les-Messieurs (Jura, France). *Archaeometry* **2016**, *58*, 930–946. [CrossRef]
38. Biron, I.; Dandridge, P.; Wypyski, M.-T. *Techniques and Materials in Limoges Enamels, in Enamels of Limoges 1100–1350*; The Met-ropolitan Museum of Art: New York, NY, USA, 1996; pp. 48–62.
39. Gratuze, B.; Soulier, I.; Blet-Lemarquand, M.; Lucy, V. De l'origine du cobalt: Du verre à la céramique. *Rev. D'archéométrie* **1996**, *20*, 77–94. [CrossRef]
40. Colomban, P.; Kırmızı, B.; Franci, G.S. Cobalt and Associated Impurities in Blue (and Green) Glass, Glaze and Enamel: Relationships between Raw Materials, Processing, Composition, Phases and International Trade. *Minerals* **2021**, *11*, 633. [CrossRef]
41. Calligaro, T.; Périn, P.; Vallet, F.; Poirot, J.-P. Contribution à l'étude des grenats mérovingiens (Basilique de Saint-Denis et autres collections du musée d'Archéologie nationale, diverses collections publiques et objets de fouilles récents). *Antiq. Natl.* **2007**, *38*, 111–144.
42. Aurisicchio, C.; Conte, A.M.; Medeghini, L.; Ottolini, L.; De Vito, C. Major and trace element geochemistry of emerald from several deposits: Implications for genetic models and classification schemes. *Ore Geol. Rev.* **2018**, *94*, 351–366. [CrossRef]
43. Gilg, H.A.; Gast, N.; Calligaro, T. Vom Karfunkelstein. *Archäologische Staatssamml.* **2010**, *37*, 87–100.
44. Greiff, S. Naturwissenschaftliche Untersuchungen zur Frage der Rohsteinquellen für frühmittelalterlichen Alman-dingranatschmuck rheinfränkischer Provenienz. *Jahrb. Römisch-Ger. Zent. Mus. Mainz* **1999**, *45*, 599–645.
45. Abu-Lughod, J.L. Before European hegemony: The World System AD 1250–1350. *Bus. Hist. Rev.* **1990**, *64*, 362–364.
46. Calligaro, T.; Périn, P. Le commerce des grenats à l'époque mérovingienne. *Archéopages* **2019**, *HS5*, 109–120.
47. Carò, F.; Schorsch, D.; Santarelli, B. Proveniencing Turquoise Artifacts from Ancient Egyptian Contexts: A Non-invasive XRF Approach. In Proceedings of the Sciences of Ancient Egyptian Materials and Technologies (SAEMT) Conference, Cairo, Egypt, 4 November 2017.
48. Ovissi, M.; Yazdi, M.; Ghorbani, M. Turquoise grading in Persian historical and modern times; a comparative study. In Proceedings of the 35th National Geosciences Conference of Geological Survey of Iran, Teheran, Iran, 18–19 February 2017; pp. 1–6.
49. Chen, Q.; Yin, Z.; Qi, L.; Xiong, Y. Turquoise from Zhushan County, Hubei Province, China. *Gems Gemol.* **2012**, *48*, 198–204. [CrossRef]
50. Pogue, J.E. *The Turquoise: A Study of Its History, Mineralogy, Geology, Ethnology, Archaeology, Mythology, Folklore and Technology*; Memoirs of the National Academy of Sciences, Cornell University Library: New York, NY, USA, 1915; 642p.
51. Amar, Z.; Lev, E. Most-Cherished Gemstones in the Medieval Arab World. *J. R. Asiat. Soc.* **2017**, *27*, 377–401. [CrossRef]
52. Shaw, I. The evidence for amethyst mining in Nubia and Egypt. *Stud. Afr. Archaeol.* **2000**, *7*, 219–227.
53. Van Roy, S. Considérations sur les pierres précieuses du XIIIe siècle au travers des œuvres d'Hugo D'Oignies conservées à Namur. *Actes Journée D'étude Hugo D'oignies Contexte Perspect. TreMa* **2011**, 205–223.
54. Howard, M.C. *Transnationalism in Ancient and Medieval Societies: The Role of Cross-Border Trade and Travel*; McFarland & Company: Jefferson, NC, USA, 2012; 289p.
55. Schumann, W. *Guides des Pierres Précieuses, Fines et Ornementales*, 3rd ed.; Delachaux et Niestlé: Paris, France, 2014; 319p.
56. Delvaux, C. L'intaille en Améthyste de Hesbaye: Étude Minéralogique et Gemmologique. Master's Thesis, University of Liège, Liège, Belgium, 2018; 60p.
57. Caucia, F.; Marinoni, L.; Leone, A.; Adamo, I. Investigation on the gemological, physical and compositional properties of some opals from Slovakia ("Hugarian" opals). *Period. Mineral.* **2013**, *82*, 251–261.
58. Rondeau, B.; Fritsch, E.; Guiraud, M.; Renac, C. Opals from Slovakia ("Hungarian" opals): A re-assessment of the conditions of formation. *Eur. J. Miner.* **2004**, *16*, 789–799. [CrossRef]